Interfacial Tensions of (H_2O + H_2) and (H_2O + CO_2 + H_2) Systems at Temperatures of (298 to 448) K and Pressures up to 45 MPa

Y. T. Florence Chow, Geoffrey C. Maitland, J. P. Martin Trusler*

Qatar Carbonates and Carbon Storage Research Centre (QCCSRC), Department of Chemical Engineering, Imperial College London, South Kensington Campus, London SW7 2AZ, United Kingdom

* Email: m.trusler@imperial.ac.uk

Abstract

We report new interfacial tension (IFT) measurements of the (H_2O + CO_2 + H_2) and (H_2O + H_2) systems at pressures of (0.5 to 45) MPa, and temperatures of (298.15 to 448.15) K, measured by the pendant-drop method. The expanded uncertainties at 95 % confidence are 0.05 K for temperature, 70 kPa for pressure, 0.017·γ for IFT in the both the binary (H_2O + H_2) system and the ternary (CO_2 + H_2 + H_2O) system. Generally, the IFT was found to decrease with both increasing pressure and increasing temperature. However, for (H_2O + H_2) at the lowest two temperatures investigated, the isothermal IFT data were found to exhibit a maximum as a function of pressure at low pressures before declining with increasing pressure. An empirical correlation has been developed for the IFT of the (H_2O + H_2) system in the full range of conditions investigated, with an average absolute deviation of 0.16 $mN \cdot m^{-1}$, and this is used to facilitate a comparison with literature values. Estimates of the IFT of the (H_2O + CO_2 + H_2) ternary system, by an empirical combining rule based on the coexisting phase compositions and the interfacial tensions of the binary systems, were found to be unsuitable at low temperatures, with an average absolute deviation of 3.6 $mN \cdot m^{-1}$ over all the conditions investigated.

Keywords: carbon dioxide; carbon storage; high pressure; interfacial tension; hydrogen; water.

Introduction

A wide range of actions is required to meet the Paris Agreement target of limiting the global average temperature increase to well below 2 °C above pre-industrial levels by 2100 [1]. Amongst there are a mix of different technological solutions including both adoption of renewable energy sources and the implementation of carbon capture and storage (CCS) technologies. CCS provides an effective means to reduce greenhouse gas emissions from large point source emitters, such as fossil fuel power plant and carbon-intensive industries. Under the 2 °C Scenario, CCS is modelled to contribute a sixth of the necessary emission reductions in 2050 [2]. At the same time, the UN's Intergovernmental Panel on Climate Change forecasts the cost of halting global warming would double without CCS [1].

Once carbon dioxide is captured from the source emitters, it is compressed, transported by ship or pipeline and then injected into an underground storage site. Suitable storage sites include deep saline aquifers, which have the greatest estimated storage capacity, depleted oil and gas reservoirs, and unmineable coal seams. High purity CO_2 from natural sources has been used industrially for decades to enhance oil recovery (EOR) from mature oil fields. For the purpose of carbon capture, it is useful to know what the effects of higher levels of impurities would be on the storage behaviour. Various impurities are expected with industrially-captured CO_2 streams, including N_2, H_2, O_2, Ar, H_2S, SO_2, NO_x, CO and CH_4 [3]. The composition of the stored CO_2 stream will depend upon the CO_2 sources feeding the storage site, the capture method, the pipeline requirements, and any identified storage limitations. Coupling hydrogen production from fossil fuels with CCS may be a favourable route to provide a decarbonised combustible fuel. In this case, hydrogen is a likely impurity in the CO_2 stream that needs to be considered.

CO_2 is injected into sedimentary formations at depths of greater than 800 m, corresponding to temperatures above 310 K and pressures above 8 MPa, in a supercritical state with density greater than 300 $kg \cdot m^{-3}$ [4]. A pressure difference is required to drive the flow of CO_2 through the reservoir formation, so the CO_2 must be pumped in at pressures higher than the surrounding reservoir fluids [5]. Typical CO_2 storage conditions involve temperatures up to 423 K with pressures up to 50 MPa [3]. The principal storage mechanisms in order of increasing time scale are: (a) structural trapping, where buoyant CO_2 is retained below impermeable caprocks; (b) capillary trapping, where CO_2 is immobilised in the pore space by means of interfacial forces; (c) solubility trapping, where the CO_2 dissolves in the reservoir fluids; and (d) mineralization, in which the CO_2 reacts to form carbonate minerals [6]. These processes can be modelled with knowledge of the fundamental thermophysical properties of relevant fluid mixtures under these extreme conditions. This aids the prediction of long-term performance of a storage project. The interfacial tension between CO_2 and reservoir fluids in the presence of impurities is fundamental for estimating the storage capacity of sedimentary formations, and for designing safe injection pressures [7]. The present paper contributes to the underpinning science in this area.

Interfacial tension (IFT) measurements involving water with various gases have been widely reported in the literature. Measurements have been made mainly by either the capillary-rise or the pendant-drop methods. The pendant drop method is preferred in more recent work, taking advantage of rapid image digitisation and automation of the axisymmetric drop shape analysis

(ADSA) for drop profile analysis. The (H_2O + CO_2) system has been studied extensively at reservoir conditions [4, 8-21]. The IFT of the (H_2O + H_2) system at T = 298 K has been reported in literature by Slowinski et al. [22], and Massoudi and King [23] up to a pressure of 10 MPa.

Various authors have reported IFT measurements of the binary systems (H_2O + N_2) [22-26], (H_2O + Ar) [23, 27], (H_2O + CO_2) [4, 17, 19, 28-30], (CO_2 + n-alkane) [31-34] and (CO_2 + brine) [17, 18, 28, 30, 35-38]. Surfactant effect on the (H_2O + CO_2) system IFTs have also been investigated [19, 39, 40]. Duchateau and Broseta [41] showed the (gas + brine) IFT to be simply related to the surface tension of the brine and the (H_2O + gas) IFT at the same pressure and temperature conditions. They found a positive linear dependence of (gas + brine) IFT on salinity. This finding concurs with the results of Li et al.'s (CO_2 + brine) IFT measurements [38]. The IFT of the ternary mixture (H_2O + CO_2 + N_2) has been measured by Yan et al. [25] at pressures up to 30 MPa and temperatures up to 373 K and by Chow et al. [42] at temperatures up to 448 K and pressures up to 40 MPa; the latter also studied the (H_2O + CO_2 + Ar) system [43]. The IFT of the ternary mixture (H_2O + CO_2 + H_2S), with initial gas composition of 70 mol% CO_2 and 30 mol% H_2S, have been reported by Shah et al. [7] at T = 350 K and pressures up to 15.6 MPa. They suggested an empirical combining rule for the ternary system based on a molar average of the binary system (H_2O + gas) IFTs at the same pressure and temperature. This approach was modified and tested by Chow et al. [42] on the (H_2O + CO_2 + N_2) system, with reasonable success at higher temperatures, where the difference between the two (H_2O + gas) binary system IFTs is smaller.

Various theoretical approaches to modelling the IFT of (water + gas) binary and multi-component systems have been reported in literature. Llovell et al. [44] and Georgiadis et al. [45] applied the density functional theory (DFT) combined with a molecular equation of state to model (CO_2 + hydrocarbon) and (H_2O + CO_2) systems. The fully predictive model is generally able to match the experimental results, yet the computational rigour renders the method less appealing for routine calculations. A simpler gradient-theory (GT) approach combined with cubic or molecular equations of state, requires knowledge of binary 'influence' parameters specific to the components in the system: like-like influence parameters fitted to the surface tensions of the pure components; and the unlike influence parameters which can be estimated from a combining rule or fitted to experimental data. Chow et al. [43] used the SAFT-VR Mie + SGT approach to model the interfacial tensions of (H_2O + CO_2), (H_2O + N_2), (H_2O + Ar), (H_2O + CO_2 + N_2) and (H_2O + CO_2 + Ar) systems, with average absolute relative deviations of 4.2 %, 1.5 %, 1.8 %, 3.6 %, and 7.9 %, respectively.

To summarise the literature, interfacial tension measurements of the (H_2O + H_2) system has been reported by only two authors at the single temperature of 298 K and at pressures below 10 MPa. Various other (H_2O + gas) and (H_2O + CO_2 + gas) systems have been studied in the literature, involving N_2, Ar and H_2S. There are no IFT data for the (H_2O + CO_2 + H_2) system available in the literature, and filling this gap is the main focus of the present work.

Experimental Section

Apparatus.

The apparatus for carrying out pendant drop IFT measurements in corrosive environments at high temperatures (up to 473 K) and high pressures (up to 50 MPa) is shown in Fig. 1; it has been described in detail elsewhere [35]. The axisymmetric drop shape analysis (ADSA), based on integration of the Young-Laplace equation, was carried out using commercial software (Advanced DROPimage, Ramé-Hart Instrument Co.). The high pressure vessel was made from Hastelloy C-276 and was fitted with axially opposed sapphire windows. In order to regulate the temperature, the vessel was contained within an insulated aluminium jacket fitted with electric cartridge heaters and a temperature sensor, and operated with a PID temperature controller. Fluids were injected from high-pressure syringe pumps. Water was injected through a capillary tube entering the optical cell from the top, thereby forming pendant drops. A calibrated platinum resistance thermometer was inserted into an axial thermowell, bored in the wall of the view cell, for the purpose of measuring the temperature. A pressure transducer, located in the tubing external to the view cell, was used to measure the pressure. Standard uncertainties were 0.025 K for temperature and 35 kPa for pressure. The laboratory was fitted with a hydrogen-gas alarm system and the hydrogen supply cylinder was provided with a remotely-operated normally-closed solenoid valve to allow the supply to be isolated in the event of an emergency.

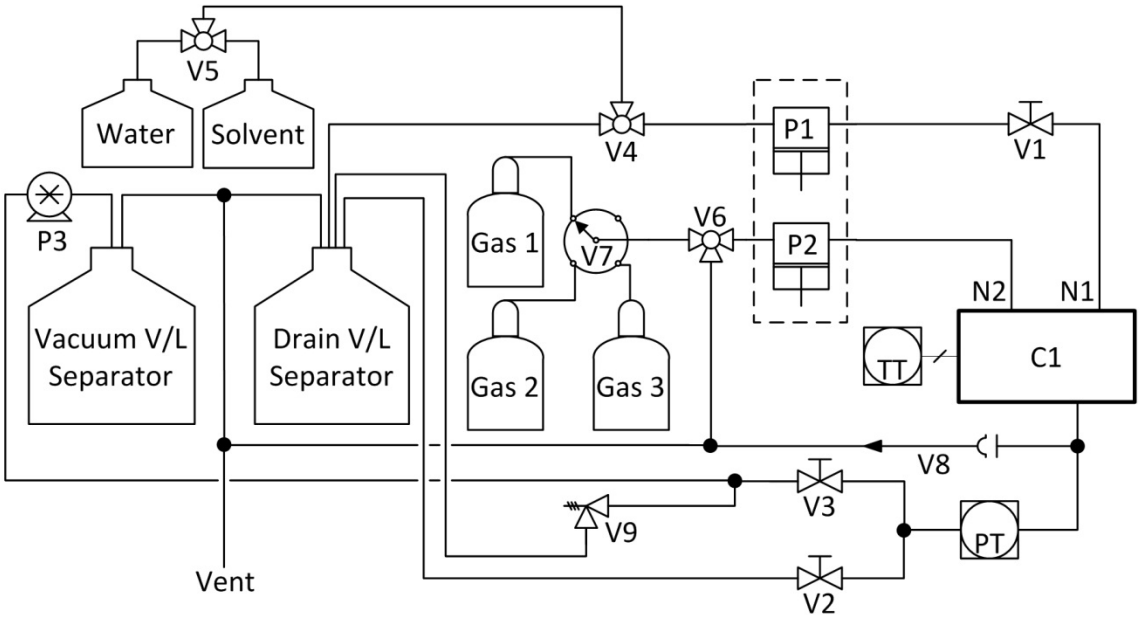

Fig. 1. Interfacial tension apparatus [35], where the gas cylinder provides pressurised pure H_2 or the (CO_2 + H_2) gas mixture to the view cell. C1: optical cell with stirrer; P1, P2: high-pressure Quizix pumps; P3: vacuum pump; TT: platinum resistance thermometer (Pt100); PT: flow-through pressure transducer; N1, N2: injection ports; V1, V2, V3: high-pressure valves; V4, V5, V6: three-way valves; V7: four-way switch; V8: rupture-disc safety head; V9: relief valve.

Materials.

The samples are described in Table 1. Pure deionised and vacuum degassed water was used. BOC supplied hydrogen with a specified mole fraction purity $x > 0.9999$ and also the binary mixture [x CO_2 + (1 - x) H_2] with x = (0.300 ± 0.015), and mole fraction of impurities less than 0.0001.

Table 1. Description of chemical samples, where x denotes mole fraction of a single substance or a mixture of defined composition and ρ_e denotes electrical resistivity.

Chemical name	Source	Purity	Additional purification
Hydrogen	BOC	$x \geq 0.9999$	None
(0.3 CO_2 + 0.7 H_2)	BOC	$x \geq 0.9999$	None
Water	Millipore Direct-Q UV3 apparatus	$\rho_e \geq 18$ MΩ·cm at T = 298 K	Vacuum degassed

Verification.

The pendant drop method is well-established, and the surface tension of water was measured at T = 298.07 K as a means of verifying correct operation of the measurement system. The surface tension was measured to be (72.1 ± 0.1) mN·m^{-1}, in close agreement with the value (71.99 ± 0.05) mN·m^{-1} obtained from the IAPWS recommended correlation by means of the REFPROP 9.1 database [46-48].

Data Analysis.

The interfacial tension was evaluated from the relation

$$\gamma = \Delta\rho g R_0^2 / \beta \,, \tag{1}$$

where $\Delta\rho$ is the density difference between the H_2O-rich and CO_2-rich phases, g is the gravitational acceleration, R_0 is the radius of curvature at the apex of the drop, and β is a dimensionless shape parameter. The parameters R_0 and β were determined from video images by the drop-shape analysis software.

For the ternary system (H_2O + CO_2 + H_2), the equilibrium-phase compositions and the density difference $\Delta\rho$ were calculated by the method described previously [42]. The solubility of the non-aqueous components in the liquid phase was calculated from an asymmetric thermodynamic model based on the Peng-Robinson (PR) equation for the gas phase and the non-random two-liquid (NRTL) model for the liquid phase with parameters fitted to experimental solubility data. The compositions of both phases were determined in flash calculations based on the combined PR-NRTL model with the overall composition constrained by the amounts of water and gas injected

into the cell. The molar volume of the aqueous phase was then obtained on the basis of the calculated composition, the partial molar volumes of the solutes, and the molar volume of pure water [47]. The partial molar volume of H_2(aq) was taken to be the value determined at T = 298.15 K by Moore et al. [49], while the partial molar volume of CO_2(aq) was obtained from the model of Sedlbauer et al. [50]. The NRTL parameter for the H_2O - CO_2 interaction were taken from [51], while those involving H_2 were set to zero. Given the extremely low solubility of H_2 in water, the latter approximation has negligible influence on the computed density difference. Tables 2 and 3 detail the other necessary parameters in the combined PR-NRTL model for solubility. The gas-phase density was calculated from the mixture model available in the REFPROP 9.1 software incorporating the equations of state of the pure components [47, 52-55].

Table 2. Thermodynamic properties of the pure components for the PR EoS where T_c is critical temperature, p_c is critical pressure and ω is acentric factor.

Component	T_c/K	p_c/MPa	ω
H_2	33.145	1.2964	–0.219
CO_2	304.13	7.3773	0.22394
H_2O	647.10	22.064	0.34430

Table 3. Binary parameters for the PR-NRTL model where T_0 = 298.15 K and T_r = T/(647.096 K)

System	Parameter Correlations	Ref.
H_2O-CO_2	$k_{ij} = 0.33810 - 0.46426(T_0/T)$ $\ln(H_{ij}/\text{MPa}) = -6.1384 + 42.842(T_0/T) - 44.358(T_0/T)^2 + 12.786(T_0/T)^3$	[51]
H_2O-H_2	$k_{ij} = \left[830.8(T_0/T)^{-1.166} - \left(\sqrt{a_i(T)}/b_i - \sqrt{a_j(T)}/b_j\right)^2\right]\left[2\sqrt{a_i(T)a_j(T)}/(b_i b_j)\right]^{-1}$	[56]
	$\ln(H_{ij}/\text{MPa}) = -\left(4.73284/T_r\right) + \left(6.08954/T_r\right)\left(1-T_r\right)^{0.355} + \left(6.06066/T_r^{0.41}\right)\exp\left(1-T_r\right) + \ln(p^{\text{sat}}_{H_2O}/\text{MPa})$	[57]
CO_2-H_2	$k_{ij} = \left[265.9(T_0/T)^{0.009} - \left(\sqrt{a_i(T)}/b_i - \sqrt{a_j(T)}/b_j\right)^2\right]\left[2\sqrt{a_i(T)a_j(T)}/(b_i b_j)\right]^{-1}$	[56]

For the binary system, the aqueous and non-aqeuous phase densities were approximated by those of the pure components and calculated from the equations of state of Wagner & Pruss [58] for water and Leachman *et al*. [55] for hydrogen. This approximation is justified on account of the extremely limited mutual solubility of the (H_2O + H_2) system. To test this further, we also estimated the density differences according to the PR-NRTL models described above. The maximum difference in $\Delta\rho$ from that based on the pure component densities was found to be 1.4 % and the average absolute difference is 0.4 %.

Results

(H_2O + H_2) system

Four isotherms at temperatures between (298 and 448) K have been measured in the (H_2O + H_2) system over a range of pressures from (0.5 to 45) MPa. The results are given in Table 4 and Fig. 2. The relative standard deviation $\sigma(\gamma)/\gamma$ of the IFT data at each state point was evaluated from 3 repeated measurements and the average was found to be 0.3 %; in all cases it was < 0.9 %. The standard relative uncertainties $u_r(\gamma)$ were calculated from the relation:

$$u_r(\gamma)^2 = \left[\frac{1}{\gamma}\left(\frac{\partial\gamma}{\partial T}\right)_p u(T)\right]^2 + \left[\frac{1}{\gamma}\left(\frac{\partial\gamma}{\partial p}\right)_T u(p)\right]^2 + \left[\frac{u(\Delta\rho)}{\Delta\rho}\right]^2 + \left[\frac{\sigma(\gamma)}{\gamma}\right]^2 \quad (2)$$

Overall, the relative uncertainty of IFT of all state points is 0.8 %, and the expanded combined relative uncertainty at 95 % confidence is 1.7 %.

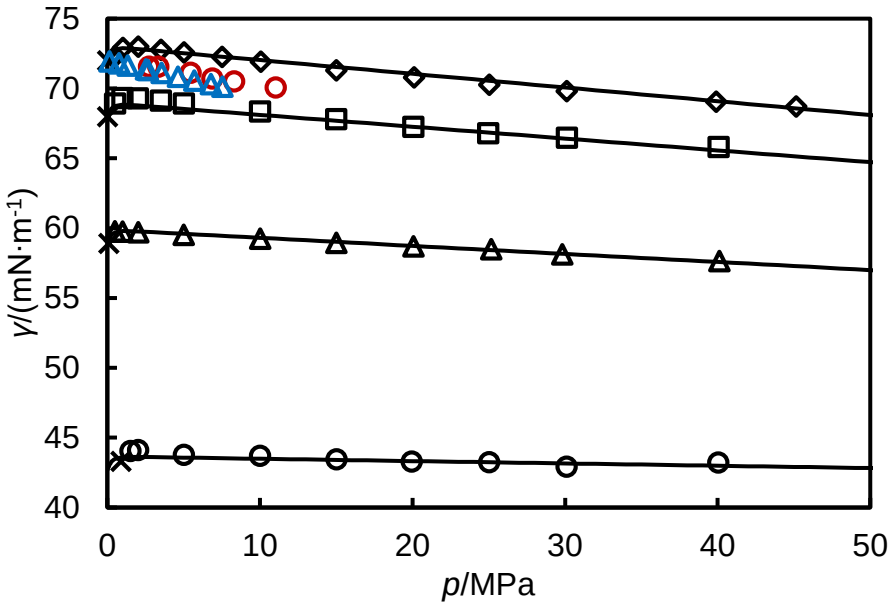

Fig. 2. Interfacial tensions γ at various pressures p for the (H_2O + H_2) system. This work: ◇, T = 298 K; □, T = 323 K; △, T = 373 K; ○, T = 448 K. Literature at T = 298 K: ○, Slowinski et al. [22]; △, Massoudi and King [23]. Calculated: – – –, equation (3); ×, pure water from REFPROP 9.1 [46, 47]

Table 4. Interfacial tension γ for (H_2O + H_2) at temperatures T and pressures p, where $\Delta\rho$ is the calculated density difference. [a,b]

p/MPa	T/K	$\Delta\rho$/(kg·m^{-3})	γ/(mN·m^{-1})	p/MPa	T/K	$\Delta\rho$/(kg·m^{-3})	γ/(mN·m^{-1})
0.5	298.03	72.3	996.8	30.1	323.02	66.5	978.4
1.0	298.03	72.9	996.5	40.1	323.00	65.8	976.4
2.0	298.04	73.0	996.1	0.5	372.74	59.8	958.5
3.5	298.05	72.8	995.4	1.0	372.77	59.7	958.3
5.0	298.04	72.6	994.7	2.0	372.78	59.7	958.0
7.5	298.04	72.2	993.6	5.0	372.87	59.5	957.1
10.1	298.04	71.9	992.6	10.0	372.81	59.3	955.9
15.0	298.06	71.3	990.7	15.0	372.73	59.0	954.7
20.1	298.06	70.8	989.0	20.1	372.85	58.7	953.6
25.0	298.04	70.3	987.5	25.2	372.77	58.5	952.7
30.1	298.06	69.8	986.2	29.8	372.77	58.1	951.9
39.9	298.09	69.1	983.9	40.1	372.78	57.6	950.5
45.2	298.05	68.7	983.0	1.5	448.04	44.0	891.9
0.5	323.02	68.9	987.8	2.0	448.02	44.1	891.9
1.0	322.90	69.3	987.7	5.0	448.24	43.8	891.5
2.0	322.98	69.3	987.2	10.0	448.29	43.7	891.2
3.5	323.00	69.1	986.6	15.0	448.28	43.4	891.0
5.0	322.99	68.9	986.0	20.0	448.33	43.3	890.8
10.0	323.00	68.3	984.2	25.0	448.31	43.2	890.7
15.0	323.00	67.8	982.5	30.1	448.31	42.9	890.6
20.0	323.01	67.2	981.0	40.1	448.35	43.2	890.4
25.0	323.01	66.8	979.7				

[a] Expanded uncertainties at 95 % confidence are $U(T)$ = 0.05 K, $U(p)$ = 70 kPa, and $U_c(\gamma)$ = 0.017γ.
[b] Density differences $\Delta\rho$ were calculated as detailed in the text

The interfacial tensions of the (H_2O + H_2) system has an unexpected behaviour whereby, at low temperatures and pressures, it initially increases with increasing pressure from the surface tension value of water, before passing through a maximum and finally adopting the expected negative gradient at higher pressures. This initial increase is observed clearly at T = (298 and 323) K, but not at the two higher temperatures, where the IFT varies more slowly with pressure. In comparison to literature results, the data at T = 298 K of Slowinski et al. [22] and Massoudi and King [23] were both systematically lower than the values measured in this work and the low-pressure maximum was not observed by these authors. The results reported by these workers were found to be consistently lower, when compared to more recent measurements, for other similar systems, such as (H_2O + N_2) [42] and (H_2O + Ar) [43].

For the purpose of interpolating the interfacial tension of the (H_2O + H_2) system, the following empirical equation was developed:

$$\gamma_{H_2O-H_2} / (\mathrm{mN \cdot m^{-1}}) = a_1 (T/\mathrm{K})^2 - a_2^{(p/\mathrm{MPa})} + a_3 (p/\mathrm{MPa}) + a_4 (T/\mathrm{K})(p/\mathrm{MPa}) + a_5 . \qquad (3)$$

This model is valid at 298 ≤ T/K ≤ 448 and 0.5 ≤ p ≤ 45 MPa, and the five parameters are listed in Table 5. The absolute average deviation Δ_{AAD} is 0.16 mN·m^{-1} for the 129 measured data points; as shown in Fig. 3, all points are fitted within their uncertainties. The systematic deviations of the data of Slowinski et al. [22] and Massoudi and King [23] are obvious in Fig. 3.

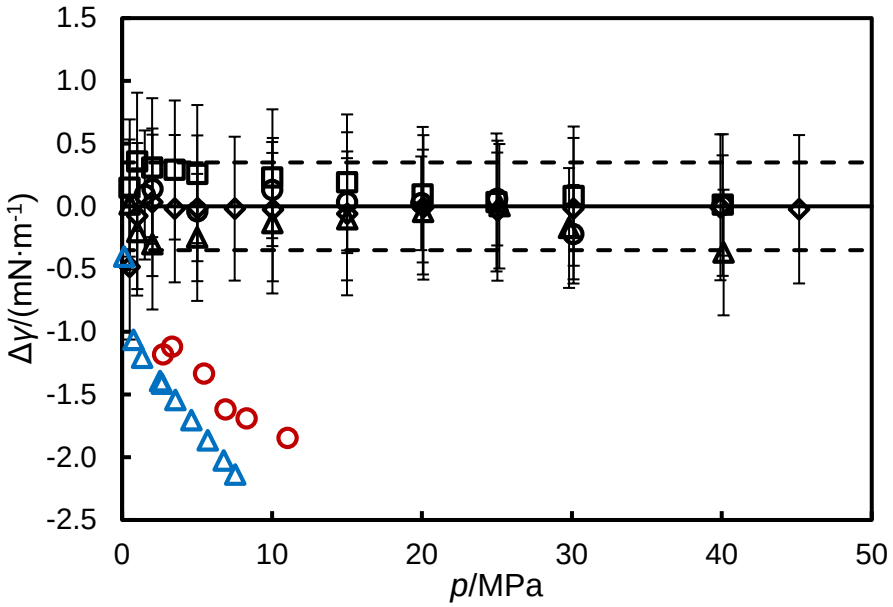

Fig. 3. Deviations $\Delta\gamma = \gamma_{exp} - \gamma_{calc}$ between experimental interfacial tensions γ_{exp} of (H_2O + H_2) and calculated values γ_{calc} from equation (3). This work: T = ◇, 298 K; T = □, 323 K; T = △, 373 K; and ○, T = 448 K. Literature at T = 298 K: ○, Slowinski et al. [22]; △, Massoudi and King [23]. Error bars show the expanded uncertainty of the measured data. Dashed lines show the absolute average deviation of the model.

Table 5. Parameters a_i of equation (3) and average absolute deviation Δ_{AAD} for the (H_2O + H_2) system.

a_1	a_2	a_3	a_4	a_5	Δ_{AAD}/(mN·m^{-1})
-2.6040	8.950 x 10^{-2}	0.2553	5.153 x 10^{-4}	96.24	0.16

(H_2O + CO_2 + H_2) system.

In the case of the (H_2O + CO_2 + H_2) system, four isotherms were measured at temperatures between (298 and 448) K at pressures from (0.5 to 45) MPa. The results are given in Table 6. The relative standard deviation $\sigma(\gamma)/\gamma$ of the IFT data at each state point was evaluated from 3 repeated measurements; the average was 0.2 %, and in all cases it was < 0.5 %. The standard relative uncertainties $u_r(\gamma)$ were calculated from equation (2) but with allowance for terms in $u(\Delta\rho)$ related to the uncertainty of the phase compositions; in particular, the estimated water level in the cell, and uncertainty of the composition of the feed gas. This led to an estimated standard uncertainty $u(\Delta\rho)/\Delta\rho$ = 1 %. However, the estimated overall combined standard relative uncertainty of the interfacial tension of all state points was unchanged at 1.7 %.

As described in the introduction, theoretical approaches based on molecular equations of state in combination with either DFT or GT are capable of describing ternary system IFTs with reasonable success. However, systems involving H_2 are complicated by quantum behaviour at low temperatures and an analysis with DFT or GT is beyond the scope of the present paper. Instead, we compare our results with the simple empirical rule suggested by Chow et al. [42] which, applied to the present systems, is:

$$\gamma_{H_2O-CO_2-H_2} = \left(y_{H_2}\gamma_{H_2O-H_2} + y_{CO_2}\gamma_{H_2O-CO_2}\right) / \left(y_{H_2} + y_{CO_2}\right), \quad (4)$$

where y denotes mole fraction in the non-aqueous phase and all IFT values pertain to the same temperature and pressure. The compositions were calculated using the PR-NRTL model and the interfacial tensions of the binary systems were evaluated from equation (3) for the (H_2O + H_2) system, and from the SAFT-VR Mie + SGT model of Chow et al. [43] for the (H_2O + CO_2) system. The predictions are compared with the experimental data in Fig. 4, where we also plot the calculated IFTs of the binary systems (H_2O + CO_2) and (H_2O + H_2). We see that the ternary-system data are in reasonable agreement with equation (4) at the two higher temperatures; however, the model fails at high pressures on the two lower isotherms. Overall the average absolute deviation of the data from equation (4) is 3.6 mN·m^{-1}. Similar results was found for the (H_2O + CO_2 + N_2) system [42]. We note that the SAFT-VR Mie + SGT model of Chow et al. [43] was not in fact superior to the empirical combination of binary IFTs in the case of the (H_2O + CO_2 + Ar) system, although much better agreement was found with SAFT-VR Mie + SGT for (H_2O + CO_2 + N_2).

Table 6. Interfacial tension γ for (H_2O + CO_2 + H_2) at temperatures T and pressures p, where $\Delta\rho$ is the calculated density difference, and x_i and y_i are the calculated aqueous- and non-aqueous-phase mole fractions respectively, with 1 = CO_2, 2 = H_2O, and 3 = H_2. [a,b]

p/MPa	T/K	$\Delta\rho$/(kg·m^{-3})	γ/(mN·m^{-1})	x_1	x_2	x_3	y_1	y_2	y_3
0.5	298.03	994.7	72.0	0.0009	0.9991	0.0000	0.2979	0.0066	0.6955
1.0	298.04	992.3	71.7	0.0017	0.9982	0.0001	0.2988	0.0034	0.6978
2.0	298.03	987.6	69.7	0.0033	0.9965	0.0002	0.2991	0.0019	0.6990
5.0	298.07	972.9	64.5	0.0072	0.9923	0.0005	0.2990	0.0010	0.7001
10.0	298.05	947.5	57.5	0.0118	0.9872	0.0010	0.2985	0.0007	0.7007
15.0	298.07	922.0	52.8	0.0148	0.9838	0.0014	0.2982	0.0007	0.7010
20.0	298.05	897.2	49.5	0.0167	0.9814	0.0019	0.2980	0.0008	0.7012
25.0	298.05	874.1	46.9	0.0180	0.9797	0.0023	0.2979	0.0009	0.7013
30.1	298.04	852.7	45.3	0.0188	0.9784	0.0027	0.2978	0.0010	0.7013
40.0	298.06	816.2	43.6	0.0199	0.9767	0.0035	0.2976	0.0011	0.7012
1.0	322.96	983.4	67.4	0.0010	0.9989	0.0001	0.2960	0.0130	0.6910
2.0	322.86	978.7	66.8	0.0020	0.9979	0.0002	0.2977	0.0069	0.6954
5.0	322.97	964.6	63.0	0.0044	0.9952	0.0004	0.2985	0.0034	0.6980
10.0	322.96	941.0	57.8	0.0075	0.9916	0.0009	0.2985	0.0024	0.6991
15.0	322.96	917.7	53.9	0.0097	0.9890	0.0013	0.2984	0.0021	0.6995
20.0	322.96	895.3	50.9	0.0113	0.9870	0.0017	0.2982	0.0021	0.6997
29.9	322.97	854.9	46.6	0.0134	0.9841	0.0025	0.2980	0.0022	0.6998
39.8	322.96	820.8	44.5	0.0146	0.9822	0.0032	0.2978	0.0024	0.6997
45.1	322.98	804.7	43.8	0.0151	0.9813	0.0036	0.2978	0.0025	0.6997
1.0	373.41	953.8	58.9	0.0005	0.9994	0.0001	0.2681	0.1062	0.6257
2.0	373.43	949.6	58.2	0.0010	0.9988	0.0002	0.2835	0.0549	0.6616
5.0	373.41	937.4	56.4	0.0024	0.9971	0.0005	0.2923	0.0249	0.6827

p/MPa	T/K	$\Delta\rho$/(kg·m^{-3})	γ/(mN·m^{-1})	x_1	x_2	x_3	y_1	y_2	y_3
10.0	373.44	917.0	53.2	0.0044	0.9947	0.0009	0.2951	0.0151	0.6898
15.0	373.44	897.3	50.3	0.0059	0.9927	0.0014	0.2959	0.0120	0.6921
20.0	373.32	878.4	48.3	0.0072	0.9909	0.0019	0.2962	0.0105	0.6933
30.0	373.32	843.6	45.0	0.0092	0.9881	0.0027	0.2964	0.0094	0.6943
40.1	373.33	813.0	43.1	0.0106	0.9859	0.0035	0.2964	0.0089	0.6947
2.0	448.25	884.7	43.4	0.0005	0.9993	0.0002	0.1645	0.4515	0.3840
5.0	448.21	873.6	42.8	0.0017	0.9977	0.0006	0.2413	0.1954	0.5632
10.0	448.29	857.5	41.0	0.0034	0.9952	0.0014	0.2676	0.1080	0.6245
15.0	448.47	841.5	39.3	0.0049	0.9929	0.0022	0.2762	0.0789	0.6450
20.0	448.58	826.3	37.9	0.0062	0.9908	0.0029	0.2805	0.0642	0.6553
25.1	448.67	811.8	36.8	0.0074	0.9889	0.0036	0.2830	0.0553	0.6616
30.0	448.78	798.4	35.9	0.0084	0.9872	0.0043	0.2847	0.0496	0.6657
40.1	448.79	773.0	34.0	0.0102	0.9841	0.0057	0.2868	0.0419	0.6712
44.7	448.87	762.5	33.3	0.0109	0.9828	0.0063	0.2875	0.0396	0.6729

[a] Expanded uncertainties at 95 % confidence are $U(T) = 0.05$ K, $U(p) = 70$ kPa, and $U_c(\gamma) = 0.017\gamma$.
[b] Density differences $\Delta\rho$ and phase compositions x_i and y_i were calculated as detailed in the text.

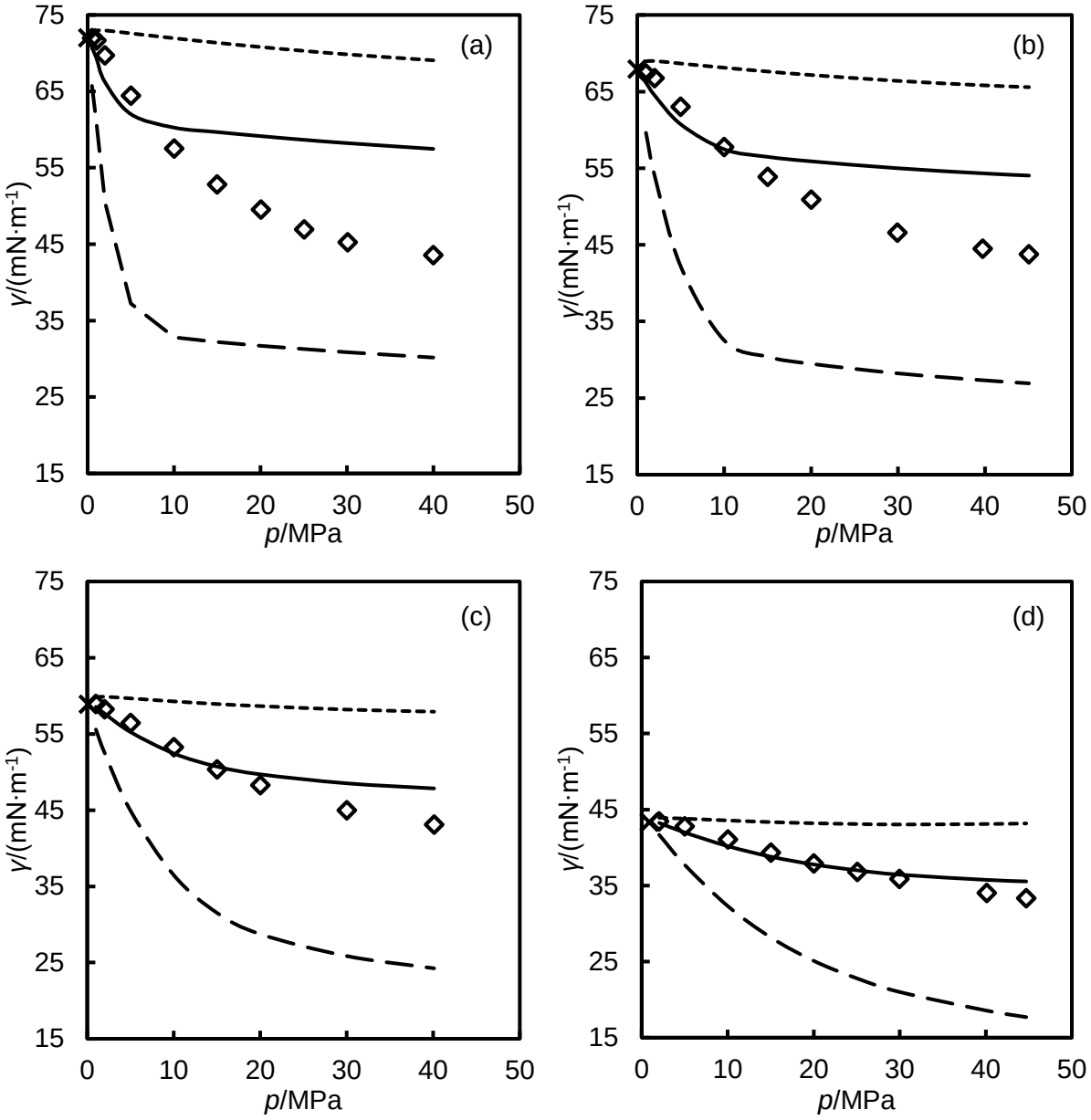

Fig. 4. Interfacial tensions γ of (H_2O + H_2 + CO_2) at various pressures p and gas-phase mole fractions y_{CO_2} of CO_2: ◇, measured values with y_{CO_2} = 0.300; — —, calculated values for y_{CO_2} = 1 from the SAFT-VR Mie + SGT model of Chow et al. [43]; – – –, calculated values for y_{CO_2} = 0 from equation (3); ——, predicted values for calculated values from equation (4) for y_{CO_2} = 0.3. (a) T = 298 K, (b) T = 323 K, (c) T = 373 K, (d) T = 448 K.

Conclusion

Interfacial tension measurements of the (H_2O + CO_2 + H_2) and (H_2O + H_2) systems are reported at pressures of (0.5 to 45) MPa and temperatures of (298.15 to 448.15) K. The results show that H_2 as an impurity will increase the IFT between CO_2-rich and H_2O-rich phases, in turn slightly increasing the pressure required to displace brine from the pore-space in aquifer storage. Increases in IFT will tend to improve capillary trapping and reduce penetration of cap rocks.

An accurate empirical correlation for interfacial tension has been developed for the (H_2O + H_2) system in the range of conditions investigated. Finally, predictions of the interfacial tension of the (H_2O + CO_2 + H_2) system, based on a simple combination of the interfacial tensions of the two binary system, have been examined. These predictions were found to be unsatisfactory at low temperatures and high pressures. Future work might address this deficiency by means of a density gradient model, ideally implemented for multicomponent mixtures comprising CO_2, H_2O and common impurity gases.

Acknowledgements

This work was carried out as part of the Qatar Carbonates and Carbon Storage Research Centre (QCCSRC). We gratefully acknowledge the funding of QCCSRC provided jointly by Qatar Petroleum, Shell, and the Qatar Science & Technology Park, and for supporting the present project, and the permission to publish this research.

References

[1] Adoption of the Paris Agreement. Proposal by the President. , in: Conference of the Parties Twenty-first session, Paris, 2015.
[2] IEA, Energy Technology Perspectives, in, IEA, 2012.
[3] H. Li, J.P. Jakobsen, Ø. Wilhelmsen, J. Yan, PVTxy properties of CO_2 mixtures relevant for CO_2 capture, transport and storage: Review of available experimental data and theoretical models, Appl. Energy, 88 (2011) 3567-3579.
[4] A. Georgiadis, G. Maitland, J.P.M. Trusler, A. Bismarck, Interfacial Tension Measurements of the (H_2O + CO_2) System at Elevated Pressures and Temperatures, Journal of Chemical & Engineering Data, 55 (2010) 4168–4175.
[5] P. Olden, G. Pickup, M. Jin, E. Mackay, S. Hamilton, J. Somerville, A. Todd, Use of rock mechanics laboratory data in geomechanical modelling to increase confidence in CO_2 geological storage, Int.J. Greenhouse Gas Control, 11 (2012) 304-315.
[6] B. Metz, O. Davidson, H. de Coninck, M.L.L. Meyer, Special Report on Carbon Dioxide Capture and Storage, in, IPCC, Cambridge, U.K, 2005.
[7] V. Shah, D. Broseta, G. Mouronval, F. Montel, Water/acid gas interfacial tensions and their impact on acid gas geological storage, International Journal of Greenhouse Gas Control, 2 (2008) 594-604.
[8] E.W. Hough, G.J. Heuer, J.W. Walker, An Improved Pendant Drop, Interfacial Tension Apparatus and Data for Carbon Dioxide and Water, AIME Petroleum Transactions, 216 (1959) 469-472.

[9] R. Massoudi, A.D. King, Effect of pressure on surface-tension of water - adsorption of low-molecular weight gases on water at 25 degrees, J. Phys. Chem., 78 (1974) 2262-2266.
[10] C. Jho, D. Nealon, S. Shogbola, A.D. King, Effect of pressure on surface-tension of water - adsorption of hydrocarbon gases and carbon-dioxide on water at temperatures between 0 C and 50 C, J. Colloid Interface Sci., 65 (1978) 141-154.
[11] B.S. Chun, G.T. Wilkinson, Interfacial-tension in high-pressure carbon-dioxide mixtures, Ind. Eng. Chem. Res., 34 (1995) 4371-4377.
[12] A. Wesch, N. Dahmen, K. Ebert, J. Schon, Interfacial tension, drop size, and angle of contact in the H_2O/CO_2 binary system at temperatures of 298-333 K and pressures up to 30 MPa, Chem. Ing. Tech., 69 (1997) 942-946.
[13] S.R.P. da Rocha, K.L. Harrison, K.P. Johnston, Effect of surfactants on the interfacial tension and emulsion formation between water and carbon dioxide, Langmuir, 15 (1999) 419-428.
[14] A. Hebach, A. Oberhof, N. Dahmen, A. Kogel, H. Ederer, E. Dinjus, Interfacial tension at elevated pressures - measurements and correlations in the water plus carbon dioxide system, J. Chem. Eng. Data, 47 (2002) 1540-1546.
[15] F. Tewes, F. Boury, Thermodynamic and dynamic interfacial properties of binary carbon dioxide-water systems, J. Phys. Chem. B, 108 (2004) 2405-2412.
[16] J.Y. Park, J.S. Lim, C.H. Yoon, C.H. Lee, K.P. Park, Effect of a fluorinated sodium bis(2-ethylhexyl) sulfosuccinate (aerosol-OT, AOT) analogue surfactant on the interfacial tension of CO_2 plus water and CO_2 plus Ni-plating solution in near- and supercritical CO_2, J. Chem. Eng. Data, 50 (2005) 299-308.
[17] P. Chiquet, J.-L. Daridon, D. Broseta, S. Thibeau, CO_2/water interfacial tensions under pressure and temperature conditions of CO_2 geological storage, Energy Conversion and Management, 48 (2007) 736-744.
[18] C. Chalbaud, M. Robin, J.M. Lombard, F. Martin, P. Egermann, H. Bertin, Interfacial tension measurements and wettability evaluation for geological CO_2 storage, Adv. Wat. Resour., 32 (2009) 98-109.
[19] T. Akutsu, Y. Yamaji, H. Yamaguchi, M. Watanabe, R.L. Smith, H. Inomata, Interfacial tension between water and high pressure CO_2 in the presence of hydrocarbon surfactants, Fluid Phase Equilibria, 257 (2007) 163-168.
[20] S. Bachu, D.B. Bennion, Interfacial tension between CO_2, freshwater, and brine in the range of pressure from (2 to 27) MPa, temperature from (20 to 125) degrees C, and water salinity from (0 to 334 000) $mg.L^{-1}$, J. Chem. Eng. Data, 54 (2009) 765-775.
[21] Y. Sutjiadi-Sia, P. Jaeger, R. Eggers, Interfacial phenomena of aqueous systems in dense carbon dioxide, J. Supercrit. Fluids, 46 (2008) 272-279.
[22] E.J.J. Slowinski, E.E. Gates, C.E. Waring, The Effect of Pressure on the Surface Tensions of Liquids, J. Phys. Chem., 61 (1957) 808-810.
[23] R. Massoudi, A.D.J. King, Effect of Pressure on the Surface Tension of Water. Adsorption of Low Molecular Weight Gases on Water at 25°, J. Phys. Chem., 78 (1974) 2262-2266.
[24] G. Wiegand, E.U. Franck, Interfacial tension between water and non-polar fluids up to 473 K and 2800 bar, Berichte der Bunsengesellschaft für physikalische Chemie, 98 (1994) 809–817.
[25] W. Yan, G.-Y. Zhao, G.-J. Chen, T.-M. Guo, Interfacial Tension of (Methane + Nitrogen) + Water and (Carbon Dioxide + Nitrogen) + Water Systems, Journal of Chemical & Engineering Data, 46 (2001) 1544-1548.
[26] Y.-L. Tian, Y.-F. Xiao, H.-X. Zhu, D. Xi-Jing, R. Xiao-Wen, Z. Feng-Cai, Interfacial Tensions between Water and Non-polar Fluids at High Pressures and High Temperatures, Acta Physico-Chimica Sinica, 13 (1997) 89-95.
[27] G. Wiegand, E.U. Franck, Interfacial tension between water and non-polar fluids up to 473 K and 2800 bar, Ber. Bunsenges. Phys. Chem. , 98 (1994) 809–817.
[28] S. Bachu, D. Brant Bennion, Dependence of CO_2-brine interfacial tension on aquifer pressure, temperature and water salinity, Energy Procedia, 1 (2009) 3157-3164.

[29] B. Kvamme, T. Kuznetsova, A. Hebach, A. Oberhof, E. Lunde, Measurements and modelling of interfacial tension for water+carbon dioxide systems at elevated pressures, Computational Materials Science, 38 (2007) 506-513.
[30] S. Bachu, D.B. Bennion, Interfacial Tension between CO_2, Freshwater, and Brine in the Range of Pressure from (2 to 27) MPa, Temperature from (20 to 125) °C, and Water Salinity from (0 to 334 000) $mg \cdot L^{-1}$, J. Chem. Eng. Data, 54 (2009) 765–775.
[31] P.T. Jaeger, R. Eggers, Interfacial properties at elevated pressures in reservoir systems containing compressed or supercritical carbon dioxide, The Journal of Supercritical Fluids, 66 (2012) 80-85.
[32] O.G. Niño Amézquita, S. Enders, P.T. Jaeger, R. Eggers, Interfacial properties of mixtures containing supercritical gases, The Journal of Supercritical Fluids, 55 (2010) 724-734.
[33] A. Georgiadis, F. Llovell, A. Bismarck, F.J. Blas, A. Galindo, G.C. Maitland, J.P.M. Trusler, G. Jackson, Interfacial tension measurements and modelling of (carbon dioxide+n-alkane) and (carbon dioxide+water) binary mixtures at elevated pressures and temperatures, The Journal of Supercritical Fluids, 55 (2010) 743-754.
[34] R.D. Shaver, R.L. Robinson Jr., K.A.M. Gasem, An automated apparatus for equilibrium phase compositions, densities, and interfacial tensions: data for carbon dioxide + decane, Fluid Phase Equilib., 179 (2001) 43-66.
[35] X. Li, E. Boek, G.C. Maitland, J.P.M. Trusler, Interfacial Tension of (Brines + CO_2): (0.864 NaCl + 0.136 KCl) at Temperatures between (298 and 448) K, Pressures between (2 and 50) MPa, and Total Molalities of (1 to 5) $mol \cdot kg^{-1}$, Journal of Chemical & Engineering Data, 57 (2012) 1078-1088.
[36] C.A. Aggelopoulos, M. Robin, O. Vizika, Interfacial tension between CO_2 and brine ($NaCl+CaCl_2$) at elevated pressures and temperatures: The additive effect of different salts, Adv. Wat. Resour., 34 (2011) 505-511.
[37] C.A. Aggelopoulos, M. Robin, E. Perfetti, O. Vizika, $CO_2/CaCl_2$ solution interfacial tensions under CO_2 geological storage conditions: Influence of cation valence on interfacial tension, Adv. Wat. Resour., 33 (2010) 691-697.
[38] R.D. Chirico, T.W. de Loos, J. Gmehling, A.R.H. Goodwin, S. Gupta, W.M. Haynes, K.N. Marsh, V. Rives, J.D. Olson, C. Spencer, J.F. Brennecke, J.P.M. Trusler, Guidelines for reporting of phase equilibrium measurements (IUPAC Recommendations 2012), Pure appl. Chem., 84 (2012) 1785-1813.
[39] F. Tewes, F. Boury, Dynamic and rheological properties of classic and macromolecular surfactant at the supercritical CO_2–H_2O interface, The Journal of Supercritical Fluids, 37 (2006) 375-383.
[40] V.V. Dhanuka, J.L. Dickson, W. Ryoo, K.P. Johnston, High internal phase CO_2-in-water emulsions stabilized with a branched nonionic hydrocarbon surfactant, J. Colloid Interface Sci., 298 (2006) 406-418.
[41] C. Duchateau, D. Broseta, A simple method for determining brine-gas interfacial tensions, Adv. Wat. Resour., 42 (2012) 30-36.
[42] Y.T.F. Chow, G.C. Maitland, J.P.M. Trusler, Interfacial tensions of the (CO_2 + N_2 + H_2O) system at temperatures of (298 to 448) K and pressures up to 40 MPa, J. Chem. Thermodyn., 93 (2016) 392-403.
[43] Y.T.F. Chow, D.K. Eriksen, A. Galindo, A.J. Haslam, G. Jackson, G.C. Maitland, J.P.M. Trusler, Interfacial Tensions of Systems Comprising Water, Carbon Dioxide and Diluent Gases at High Pressures: Experimental Measurements and Modelling with SAFT-VR Mie and Square-Gradient Theory, Fluid Phase Equilib., 407 (2016) 159-176.
[44] F. Llovell, N. Mac Dowell, F.J. Blas, A. Galindo, G. Jackson, Application of the SAFT-VR density functional theory to the prediction of the interfacial properties of mixtures of relevance to reservoir engineering, Fluid Phase Equilib., 336 (2012) 137-150.

[45] A. Georgiadis, F. Llovell, A. Bismarck, F.J. Blas, A. Galindo, G.C. Maitland, J.P.M. Trusler, G. Jackson, Interfacial tension measurements and modelling of (carbon dioxide+n-alkane) and (carbon dioxide+water) binary mixtures at elevated pressures and temperatures, Journal of Supercritical Fluids, 55 (2010) 743-754.
[46] E.W. Lemmon, M.L. Huber, M.O. McLinden, NIST Standard Reference Database 23: Reference Fluid Thermodynamic and Transport Properties-REFPROP, Version 9.1, in, National Institute of Standards and Technology, Standard Reference Data Program, Gaithersburg, 2013.
[47] W. Wagner, A. Pruss, The IAPWS formulation 1995 for the thermodynamic properties of ordinary water substance for general and scientific use, J. Phys. Chem. Ref. Data, 31 (2002) 387-535.
[48] International Association for the Properties of Water and Steam, Release on the surface tension of ordinary water substance, Physical Chemistry of Aqueous Systems, in: 12th International Conference on the Properties of Water and Steam, Orlando, Florida, 1994, pp. A139-A142.
[49] J.C. Moore, R. Battino, T.R. Rettich, Y.P. Handa, E. Wilhelm, Partial Molar Volumes of "Gases" at Infinite Dilution in Water at 29815 K, J. Chem. Eng. Data 27 (1982) 22-24.
[50] J. Sedlbauer, J.P. O'Connell, R.H. Wood, A new equation of state for correlation and prediction of standard molal thermodynamic properties of aqueous species at high temperatures and pressures, Chem. Geol., 163 (2000) 43-63.
[51] S.-X. Hou, G.C. Maitland, J.P.M. Trusler, Measurement and modeling of the phase behavior of the (carbon dioxide+water) mixture at temperatures from 298.15K to 448.15K, J Supercrit Fluid, 73 (2013) 87-96.
[52] E.W. Lemmon, M.L. Huber, M.O. McLinden, NIST standard reference database 23: Reference fluid thermodynamic and transport properties - REFPROP, Version 9.1, in, National Institute of Standards and Technology Gaithersburg, 2013.
[53] R. Span, W. Wagner, A new equation of state for carbon dioxide covering the fluid region from the triple-point temperature to 1100 K at pressures up to 800 MPa, J. Phys. Chem. Ref. Data, 25 (1996) 1509-1596.
[54] O. Kunz, W. Wagner, The GERG-2008 wide-range equation of state for natural gases and other mixtures: an expansion of GERG-2004, J. Chem. Eng. Data, 57 (2012) 3032–3091.
[55] J.W. Leachman, R.T. Jacobsen, S.G. Penoncello, E.W. Lemmon, Fundamental Equations of State for Parahydrogen, Normal Hydrogen, and Orthohydrogen, J. Phys. Chem. Ref. Data, 38 (2009) 721-748.
[56] R. Privat, J.-N. Jaubert, Predicting the Phase Equilibria of Carbon Dioxide Containing Mixtures Involved in CCS Processes Using the PPR78 Model, (2014).
[57] R. Fernández-Prini, J.L. Alvarez, A.H. Harvey, Henry's Constants and Vapor–Liquid Distribution Constants for Gaseous Solutes in H_2O and D_2O at High Temperatures, J. Phys. Chem. Ref. Data 32 (2003) 903.
[58] W. Wagner, A. Pruss, The IAPWS Formulation 1995 for the Thermodynamic Properties of Ordinary Water Substance for General and Scientific Use, J. Phys. Chem. Ref. Data, 31 (2002) 387-535.